IEEE Access
Multidisciplinary ⋮ Rapid Review ⋮ Open Access Journal

Received 1 December 2022, accepted 15 December 2022, date of publication 22 December 2022,
date of current version 29 December 2022.

Digital Object Identifier 10.1109/ACCESS.2022.3231609

RESEARCH ARTICLE

Variable Structure Control of Second Order Systems With Nonlinear Uncertain Discontinuous Input Functions Using Approximate Inverses

DENIS VASKO, JÁN KARDOŠ, AND EVA MIKLOVIČOVÁ
Faculty of Electrical Engineering and Information Technology, Institute of Robotics and Cybernetics, Slovak University of Technology in Bratislava, 812 19 Bratislava, Slovakia

Corresponding author: Denis Vasko (denis.vasko@stuba.sk)

This work was supported by the Agency of Ministry of Education and Academy of Science of Slovak Republic Scientific grant agency [Vedecká grantová agentúra (VEGA)] under Grant 1/0049/20.

ABSTRACT We consider second order nonlinear systems in control canonical form, where the functional relation between the control variable and the system acceleration is nonlinear, uncertain and discontinuous. We approximate the nonlinear uncertain and discontinuous function with an invertible one, and use variable structure control theory to suppress the error of the approximate inverse. We rewrite the finite time reaching law or the terminal reaching law into the form of inequalities and use these inequalities to design a control law that drives the system state to the sliding surface in finite time, and one that ensures the convergence of the system speed and position errors to a narrow, adjustable width band around zero. The stability of the control system is also analyzed and proven. We demonstrate how to ensure the sufficiency of the available control effort, by the proper design of control parameters. The method is then validated on a numerical model of a nonlinear system with nonlinear, uncertain and discontinuous input function.

INDEX TERMS Variable structure control, sliding mode control, reaching law, nonlinear control, nonlinear system.

I. INTRODUCTION

The disturbance rejection property of sliding mode control of second order systems has already been widely emphasized in many publications and applications. Many of these previous works assume an affine relation between the control variable and the system acceleration [1], [2], [3], [4], [5], [6].

We consider cases where the functional relation between the control variable and the system acceleration, i.e. the input function, is not affine. In such cases, if the input function is invertible, then the inverse can be used to achieve the specified control effort, or the system can be linearized. If the first method is used, then parameter uncertainties worsen the system's performance, as the inverse will become imprecise. On the other hand, if linearization is used, then additional analysis is required to verify that the linearized system meets the stability and performance requirements.

The associate editor coordinating the review of this manuscript and approving it for publication was Zheng Chen.

We propose a different method. This method does not rely on the invertibility of the input function, rather, it allows the designer to specify the shape of the input function and perform the controller design with this new input function, provided that certain conditions are satisfied. The differences between the real and the specified input functions are taken into account by the variable structure control algorithm.

This context of using variable structure control is atypical, as the disturbance is self-inflicted. However, the traditional external disturbance can also be factored into the design, this important property is preserved.

This method allows the control of systems with nonlinear uncertain discontinuous input functions and the controller design can happen as if the input function was continuous and invertible. This property is demonstrated in this paper using a case study.

In the next parts of this paper we will define partial inverses, derive some of their properties, state the system model, discuss the conditions of controllability for the given

second order system and derive a finite time reaching exponentially stable (linear) sliding mode control law. We test the controller on a second order nonlinear system with a nonlinear uncertain discontinuous input function.

II. PARTIAL INVERSES AND FORWARD ERRORS

In the following we define the notion of partial inverses and state and prove some of their properties.

Definition 1: Let $h(u)$, $g(u)$ and $\xi(u)$ be scalar functions, such that

$$h(u) = g(u) + \xi(u) \tag{1}$$

where $g(u)$ is strictly monotonic and the range of $g(u)$ is the domain of $g^{-1}(a)$ and vice versa. Then, we will call $g(u)$ an invertible part of $h(u)$, $g^{-1}(a)$ a partial inverse of $h(u)$ and $\xi(u)$ is the error of the invertible part $g(u)$, or the forward error.

Analogues to the following lemmas can be derived for strictly decreasing $g(u)$ as well, but we will assume that $g(u)$ is strictly increasing.

Lemma 1: If $g(u)$ is an invertible part of $h(u)$, $g(u)$ is strictly increasing, $k(t)$ is a function such that $k(t) - \xi(u)$ is in the range of $g(u)$, then:

1) $u(t) = g^{-1}(k(t) - \xi(u)) \implies h(u) = k(t)$

If $|\xi(u)| < \xi_{max}$, i.e. $\xi(u)$ is bounded, and $u(t)$ is in the domain of g, then:

2) *If $k(t) + \xi_{max}$ is in the range of g, we have*
   $u(t) \geq g^{-1}(k(t) + \xi_{max}) \implies h(u) \geq k(t)$
3) *If $k(t) - \xi_{max}$ is in the range of g, we have*
   $u(t) \leq g^{-1}(k(t) - \xi_{max}) \implies h(u) \leq k(t)$

Proof: The first property is easily verified from Definition 1. The second and third properties require g to be strictly increasing.

Let us prove the second property in Lemma 1. Assume that $k(t)+\xi_{max}$ is in the range of g. Then, since the range of g is the domain of g^{-1}, the value $k(t)+\xi_{max}$ is in the domain of g^{-1}. Let

$$u(t) \geq g^{-1}(k(t) + \xi_{max}) \,. \tag{2}$$

Assume that $u(t)$ is in the domain of g and observe that the value of $g^{-1}(k(t) + \xi_{max})$ is in the domain of g, since the domain of g is the range of g^{-1}. This allows us to apply g on (2) and get

$$g(u) \geq k(t) + \xi_{max} \,, \tag{3}$$

where we used the fact that g is increasing. Using (1), we have

$$h(u) = g(u) + \xi(u) \geq k(t) + \xi_{max} + \xi(u) \geq k(t) \,. \tag{4}$$

The proof of the third property is similar. □

The nonlinear equation in part 1) of Lemma 1 is difficult to solve in general, since u appears on both sides of this equation. However, the inequalities in part 2) and 3) of Lemma 1 are easier to satisfy, since the right side is not a function of the control effort u.

The smaller ξ_{max} is, the better inverse is $g^{-1}(a)$ to $h(u)$. The optimal partial inverse $g_*^{-1}(a)$ to $h(u)$ is the one that minimizes $\xi_{max} = \max_u |\xi(u)|$.

III. THE PLANT

We will use Lemma 1 and the general theory of variable structure control systems to design a controller for the second order nonlinear system described by (5)

$$\ddot{x}(t) = f(\boldsymbol{x}) + h(u) + \eta(t) \,, \tag{5}$$

where $\ddot{x}(t)$ is the system's acceleration, $\dot{x}(t)$ the system's speed, $x(t)$ is its position, $f(\boldsymbol{x})$ is some known function of the system state $\boldsymbol{x}(t)$, $h(u)$ is the input function and $\eta(t)$ is a bounded disturbance with $|\eta(t)| \leq \eta_{max}$.

To control (5), one can design a controller for the affine system

$$\ddot{x}(t) = f(\boldsymbol{x}) + v(t) + \eta(t) \,, \tag{6}$$

where $v(t)$ is the control input of the affine system, and use $u(t) = h^{-1}(v)$ in (5). This approach fails if h^{-1} is not invertible. However, we can still use the method developed in the next section, if $h(u)$ satisfies certain conditions.

IV. CONTROLLABILITY AND DISCONTINUOUS CONTROL

We will use Lemma 1 to prove Lemma 2, which is given bellow. Lemma 2 shows that we can control $\text{sign}[\ddot{x}(t)]$ and set a lower bound of $|\ddot{x}(t)|$ if a certain set of conditions is satisfied.

Lemma 2: Consider the dynamic system described by (5). If $g(u)$ is an invertible part of $h(u)$ with the bounded forward error $\xi(u)$, where $\xi_{max} > |\xi(u)|$, then if

$$d^+(\boldsymbol{x}, t) = -f(\boldsymbol{x}) + \xi_{max} + \eta_{max} + \ddot{x}_t(t) \tag{7}$$

is in the range of g and $u(t)$ is in the domain of g, then

$$u(t) \geq g^{-1}(d^+) \implies \ddot{x}(t) \geq \ddot{x}_t(t) \,, \tag{8}$$

where $\ddot{x}_t(t)$ is the target minimal acceleration. Also, if

$$d^-(\boldsymbol{x}, t) = -f(\boldsymbol{x}) - \xi_{max} - \eta_{max} + \ddot{x}_t(t) \tag{9}$$

is in the range of g and $u(t)$ is in the domain of g, then

$$u(t) \leq g^{-1}(d^-) \implies \ddot{x}(t) \leq \ddot{x}_t(t) \,. \tag{10}$$

Proof: To prove (8), apply case 2) of Lemma 1 with

$$k(t) = d^+(\boldsymbol{x}, t) - \xi_{max} \,, \tag{11}$$

based on which we get

$$u(t) \geq g^{-1}[d^+(\boldsymbol{x}, t)] \implies h(u) \geq d^+(\boldsymbol{x}, t) - \xi_{max} \tag{12}$$

and by (7) we also have

$$d^+(\boldsymbol{x}, t) - \xi_{max} = -f(\boldsymbol{x}) + \ddot{x}_t(t) + \eta_{max} \,. \tag{13}$$

Therefore (12) can be rewritten as

$$\begin{aligned} u(t) \quad &\geq \quad g^{-1}[d^+(\boldsymbol{x}, t)] \\ &\implies h(u) \geq -f(\boldsymbol{x}) + \ddot{x}_t(t) + \eta_{max} \,. \end{aligned} \tag{14}$$

But if

$$h(u) \geq -f(\boldsymbol{x}) + \ddot{x}_t(t) + \eta_{max} \tag{15}$$

then

$$f(\boldsymbol{x}) + h(u) + \eta(t) \geq \ddot{x}_t(t) + \eta_{max} + \eta(t) \geq \ddot{x}_t(t)\,, \tag{16}$$

which proves (8). The proof of (10) is simliar. □

The fact that we can set $\ddot{x}(t)$ to be smaller or greater than $\ddot{x}_t(t)$ allows us to control the sign$[\ddot{x}(t)]$ and set a lower bound for the magnitude of $|\ddot{x}(t)|$. Note, that Lemma 2 explicitly states that $d^+(\boldsymbol{x}, t)$ and $d^-(\boldsymbol{x}, t)$ must be in the range of g.

V. TERMINAL REACHING INEQUALITIES

The terminal reaching law has already been studied in many publications [3], [7], [8]. Its most basic form is given by the following equation:

$$\dot{s}(\boldsymbol{e}) + K|s(\boldsymbol{e})|^{\lambda}\,\mathrm{sign}[s(\boldsymbol{e})] = 0\,, \tag{17}$$

where $s(\boldsymbol{e})$ is the switching function, $\dot{s}(\boldsymbol{e})$ is its first derivative in time, $K > 0$ and $0 < \lambda < 1$. If this equation is satisfied, then $s(\boldsymbol{e})$ converges to 0 in finite time [7], [9] given by

$$t_s = \frac{1}{K(1-\lambda)}|s(0)|^{1-\lambda}\,. \tag{18}$$

If the inequalities

$$\dot{s}(\boldsymbol{e}) \begin{cases} \leq -K|s(\boldsymbol{e})|^{\lambda} & \text{if } s(\boldsymbol{e}) > 0 \\ \geq K|s(\boldsymbol{e})|^{\lambda} & \text{if } s(\boldsymbol{e}) < 0 \end{cases} \tag{19}$$

hold, then the convergence of s to 0 is as fast or faster than in (17), for all $K > 0$ and $0 < \lambda < 1$. This statement can be proven by integrating

$$\dot{s}(\boldsymbol{e}) = -(K + \beta(t))|s(\boldsymbol{e})|^{\lambda}\,\mathrm{sign}(s) \tag{20}$$

for $\beta(t) \geq 0$ and comparing the convergence time with (18).

VI. CONTROLLER DESIGN

We design a terminal reaching exponential (linear) sliding mode controller using the lemmas derived previously for the system described by (5).

A. THE SWITCHING FUNCTION AND THE SLIDING SURFACE

Let $s(\boldsymbol{e})$ be the switching function defined by the equation

$$s(\boldsymbol{e}) = \dot{e}(t) + \alpha e(t)\,. \tag{21}$$

where $\alpha > 0$ is a constant, $e(t) = r(t) - x(t)$ is the tracking error, $r(t)$ is the reference position, $\dot{e}(t) = \dot{r}(t) - \dot{x}(t)$ is the speed error and $\dot{r}(t)$ is the reference speed. We denote the acceleration error as $\ddot{e}(t)$ and it is given by $\ddot{e}(t) = \ddot{r}(t) - \ddot{x}(t)$, where $\ddot{r}(t)$ is the reference acceleration. The control law should reduce $s(\boldsymbol{e})$ to zero, so that the compensated dynamics

$$0 = \dot{e}(t) + \alpha e(t) \tag{22}$$

is achieved.

We will often omit the arguments of $e(t)$, $\dot{e}(t)$, $\ddot{e}(t)$ and $s(\boldsymbol{e})$ and write e, $\dot{e}$, $\ddot{e}$ and s instead, for the sake of brevity and to reduce the length of expressions.

B. CONTROL LAW DESIGN

Substituting the switching function (21) into (19) we get

$$\ddot{e} + \alpha\dot{e} \begin{cases} \leq -K|s|^{\lambda} & \text{if } s > 0 \\ \geq K|s|^{\lambda} & \text{if } s < 0 \end{cases} \tag{23}$$

which is

$$\ddot{x} \begin{cases} \geq \ddot{r} + \alpha\dot{e} + K|s|^{\lambda} & \text{if } s > 0 \\ \leq \ddot{r} + \alpha\dot{e} - K|s|^{\lambda} & \text{if } s < 0 \end{cases} \tag{24}$$

where we have used the fact that $\ddot{e} = \ddot{r} - \ddot{x}$.

By Lemma 2 we have, that these conditions are satisfied by the control law $u(t)$ for which

$$\begin{aligned} u(t) &\geq g^{-1}[-f(\boldsymbol{x}) + \ddot{r} + \alpha\dot{e} + L(s)] \text{ if } s > 0 \\ u(t) &\leq g^{-1}[-f(\boldsymbol{x}) + \ddot{r} + \alpha\dot{e} - L(s)] \text{ if } s < 0 \\ L(s) &= \xi_{max} + \eta_{max} + K|s|^{\lambda} \end{aligned} \tag{25}$$

It is important to note that $-f(\boldsymbol{x}) + \ddot{r} + \alpha\dot{e} \pm L(s)$ must be in the range of g and $u(t)$ must be in the domain of g, since this is required by Lemma 2. We consider the equality case in both of these inequalities and write

$$u(t) = g^{-1}[-f(\boldsymbol{x}) + \ddot{r}(t) + \alpha\dot{e}(t) + \mathrm{sign}(s)L(s)]\,. \tag{26}$$

We insert a boundary region Ω with width Δ to avoid chattering [10]. This results in

$$u(t) = g^{-1}[-f(\boldsymbol{x}) + \ddot{r}(t) + \alpha\dot{e}(t) + \Omega(\frac{s}{\Delta})L(s)]\,, \tag{27}$$

where the function $\Omega(a)$ is defined as:

$$\Omega(a) = \sin\left[\frac{\pi}{2}\,\mathrm{sat}_1(a)\right] \tag{28}$$

and the symmetric saturation function $\mathrm{sat}_b(a)$ is defined as

$$\mathrm{sat}_b(a) = \begin{cases} a & \text{if } |a| < b \\ b\,\mathrm{sign}(a) & \text{otherwise} \end{cases} \tag{29}$$

This is a constant width boundary region, however variable width boundary regions can yield better performance [11]. The control scheme is in figure 1.

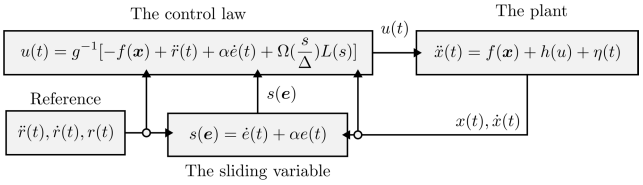

FIGURE 1. The control scheme.

C. STABILITY ANALYSIS

Since (19) holds, the reaching time is bounded by (18) when the discontinuous control law (26) is used.

Now, consider the continuous control law with a boundary layer given by (27). Since this control law is equivalent to the discontinuous one (26) for $|s| \geq \Delta$, then for initial conditions $s(0)$, that satisfy $|s(0)| \geq \Delta$, we will have

$$s \in N_\Delta = \langle -\Delta, \Delta \rangle , \tag{30}$$

after a finite time smaller than (18).

Consider the solutions of the linear first order differential equation (21) when $s \in N_\Delta$. They are [12]

$$e(t) = e(0)\epsilon^{-\alpha t} + \epsilon^{-\alpha t} \int_0^t s(\tau)\epsilon^{\alpha \tau} d\tau , \tag{31}$$

where ϵ is the standard exponential function $exp(\cdot)$. Since s is in N_Δ, we have $|s| \leq \Delta$, so

$$\left| \int_0^t s(\tau)\epsilon^{\alpha \tau} d\tau \right| \leq \int_0^t |s(\tau)|\epsilon^{\alpha \tau} d\tau \leq \int_0^t \Delta \epsilon^{\alpha \tau} d\tau , \tag{32}$$

based on the comparison property of integrals. Integrating the rightmost integral, we get

$$\left| \int_0^t s(\tau)\epsilon^{\alpha \tau} d\tau \right| \leq \frac{\Delta}{\alpha}(\epsilon^{\alpha t} - 1) , \tag{33}$$

based on which we can write

$$\left| \epsilon^{-\alpha t} \int_0^t s(\tau)\epsilon^{a \tau} d\tau \right| \leq \frac{\Delta}{\alpha}(1 - \epsilon^{-\alpha t}) \leq \frac{\Delta}{\alpha} . \tag{34}$$

Using (31) and (34) we have

$$e(0)\epsilon^{-\alpha t} - \frac{\Delta}{\alpha} \leq e(t) \leq e(0)\epsilon^{-\alpha t} + \frac{\Delta}{\alpha} \tag{35}$$

Thus, the absolute steady state error $|e(\infty)|$ is bounded by $\frac{\Delta}{\alpha}$ and it converges to this band exponentially with the time constant $\frac{1}{\alpha}$ after s converged into N_Δ.

Taking the derivative of (31) we get

$$\dot{e}(t) = -\alpha e(0)\epsilon^{-\alpha t} - \alpha \epsilon^{-\alpha t} \int_0^t s(\tau)\epsilon^{\alpha \tau} d\tau + s(t) \tag{36}$$

Using (34) we get

$$\left| \alpha \epsilon^{-\alpha t} \int_0^t s(\tau)\epsilon^{\alpha \tau} d\tau \right| \leq \Delta \tag{37}$$

Then, from (36) and (37) we have

$$-\Delta \leq \dot{e}(t) + \alpha e(0)\epsilon^{-\alpha t} - s(t) \leq \Delta \tag{38}$$

Next, using the fact that $s \in N_\Delta$ we have

$$-2\Delta \leq \dot{e}(t) + \alpha e(0)e^{-\alpha t} \leq 2\Delta . \tag{39}$$

Thus, the absolute steady state speed error $|\dot{e}(\infty)|$ is bounded by 2Δ and it approaches this band exponentially with the time constant $\frac{1}{\alpha}$ after s converged into N_Δ.

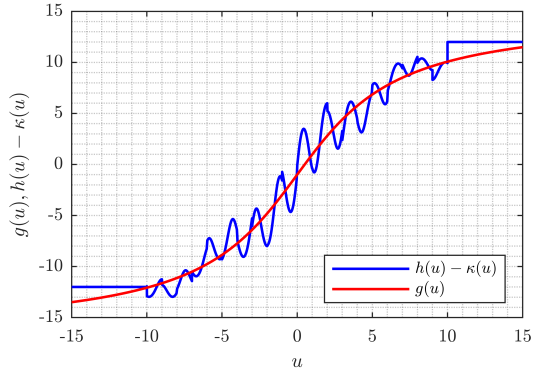

FIGURE 2. Comparison of the real input function $h(u)$ without the uncertain part $\kappa(u)$ and the invertible part $g(u)$.

VII. CONTROL TESTING

A. A NONLINEAR DISCONTINUOUS UNCERTAIN INPUT FUNCTION

Notice, that the derivation of (27) does not rely on the fact that $h(u)$ is continuous. Therefore, let us use the system

$$\ddot{x} = h(u) - \cos(\dot{x}x) + 0.01x^2 \sin(x) + 0.1\dot{x} + \eta(t) \tag{40}$$

for testing, with $\eta(t) \leq 1$. Let the input function $h(u)$ be given by

$$h(u) = -1 + 10 \operatorname{atan}[0.2u + 0.3 \sin(4u)] + \sin\lceil u \rceil + \kappa(u) \tag{41}$$

for $|u| < 10$, and by

$$h(u) = 12 \operatorname{sign}(u) + \kappa(u) \tag{42}$$

for $|u| \geq 10$. The term $\lceil u \rceil$ denotes the integer ceiling function applied to u and $\kappa(u)$ is an unknown function of input u bounded absolutely by the value 1.

B. FINDING AN INVERTIBLE PART AND EXPRESSING THE FORWARD ERROR

The first step of the design is to find an invertible part of $h(u)$ such that the forward error $\xi(u)$ is bounded. Let

$$g(u) = -1 + 10 \operatorname{atan}(0.2u) . \tag{43}$$

The comparison of $h(u) - \kappa(u)$ and $g(u)$ is in figure 2. Note that g is strictly increasing as required and its inverse is

$$g^{-1}(a) = 5 \operatorname{atan}^{-1}\left(\frac{a+1}{10}\right) . \tag{44}$$

Here $\operatorname{atan}^{-1} = \tan_{\pm\frac{\pi}{2}}$, where $\tan_{\pm\frac{\pi}{2}}$ denotes tan with its domain restricted to $\langle -\frac{\pi}{2}, \frac{\pi}{2} \rangle$.

The absolute value of the forward error $\xi(u)$ without the uncertain term $\kappa(u)$ is plotted in figure 3. We assume that it is indeed bounded by 3.8 as it appears, adding a margin for $|\kappa(u)| \leq 1$, we obtain $\xi_{max} = 4.8$.

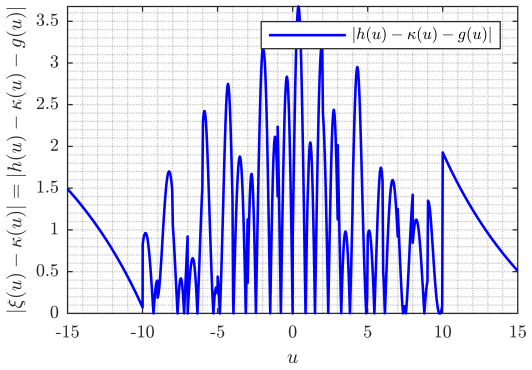

FIGURE 3. The absolute value of the forward error function $\xi(u)$ without the uncertain term $\kappa(u)$.

C. CHECKING IF THE AVAILABLE CONTROL EFFORT IS SUFFICIENT

The control law (27) is based on Lemma 2 and it requires

$$d^{\pm}(\boldsymbol{x}, t) = -f(\boldsymbol{x}) + \ddot{r}(t) + \alpha\dot{e}(t) \pm L(\boldsymbol{x}) \tag{45}$$

to be in the range of g. In this case, the range of g is

$$R(g) = \langle -1 - 5\pi, -1 + 5\pi \rangle . \tag{46}$$

Assume that $|e(0)| \leq 1$, $|\dot{e}(0)| \leq 1$, $|r| \leq 2$, $|\dot{r}| \leq 2$ and $|\ddot{r}| \leq 1$.

The value of $|s(\boldsymbol{e})|$ is bounded by $\max(|s(0)|, \Delta)$, because the control law (27) guarantees that $|s(\boldsymbol{e})|$ will be decreasing until $|s(\boldsymbol{e})| \leq \Delta$. The initial value $|s(0)|$ of $s(\boldsymbol{e})$ is therfore bounded by $\max(1 + \alpha, \Delta)$, since $s(\boldsymbol{e})$ is defined by (21) and $|e(0)| \leq 1$ as well as $|\dot{e}(0)| \leq 1$. We will choose $\Delta = 0.1$ and $\alpha = 0.94$, therefore in our case the upper bound of $|s(0)|$ is $1 + \alpha$ and not Δ.

Next, from (31) we have

$$|e(t)| \leq |e(0)| + \left| \epsilon^{-\alpha t} \int_0^t s(\tau)\epsilon^{\alpha\tau} d\tau \right| . \tag{47}$$

Using the property, that

$$\left| \epsilon^{-\alpha t} \int_0^t s(\tau)\epsilon^{\alpha\tau} d\tau \right| \leq \epsilon^{-\alpha t} \int_0^t |s(\tau)|\epsilon^{\alpha\tau} d\tau \tag{48}$$

and then, using the fact that $|s(\boldsymbol{e})|$ is bounded by $1+\alpha$, we get

$$\int_0^t |s(\tau)|\epsilon^{\alpha\tau} d\tau \leq (1 + \alpha) \int_0^t \epsilon^{\alpha\tau} d\tau . \tag{49}$$

Integrating the right side of (49) and using (48) results in

$$\left| \epsilon^{-\alpha t} \int_0^t s(\tau)\epsilon^{\alpha\tau} d\tau \right| \leq \frac{1 + \alpha}{\alpha}(1 - \epsilon^{-\alpha t}) \tag{50}$$

Using (47) and (50) we get

$$|e(t)| \leq |e(0)| + 1 + \frac{1}{\alpha} \leq 2 + \frac{1}{\alpha} \tag{51}$$

With a similar derivation based on (36) we can show that

$$|\dot{e}(t)| \leq \alpha|e(0)| + 2s(0) \leq 2 + 3\alpha . \tag{52}$$

TABLE 1. Parameters used for the numerical experiment.

α	Δ	K	ξ_{max}	η_{max}	λ
0.94	0.1	1	4.8	1	0.5

Now, since both $|r|$ and $|e|$ are bounded, then so is $|x|$ by $|e|+|r| \leq 4+\frac{1}{\alpha}$ and the same is true for $|\dot{x}|$ which is bounded by $|\dot{e}| + |\dot{r}| \leq 4 + 3\alpha$. Using these bounds we see that

$$\begin{aligned} |f(\boldsymbol{x})| &= |\cos(\dot{x}x) + 0.01x^2 \sin(x) + 0.1\dot{x}| \\ &\leq 1 + 0.01(4 + \frac{1}{\alpha})^2 + 0.1(4 + 3\alpha) \\ &\leq 1 + 0.01(16 + \frac{8}{\alpha} + \frac{1}{\alpha^2}) + 0.1(4 + 3\alpha) \\ &= 1 + 0.16 + 0.08\frac{1}{\alpha} + 0.01\frac{1}{\alpha^2} + 0.4 + 0.3\alpha \\ &= 1.56 + 0.3\alpha + 0.08\frac{1}{\alpha} + 0.01\frac{1}{\alpha^2} \end{aligned} \tag{53}$$

and that

$$\begin{aligned} L(\boldsymbol{x}) &= \xi_{max} + \eta_{max} + K|s(\boldsymbol{x})|^{\lambda} \\ &\leq 4.8 + 1 + K|1 + \alpha|^{\lambda} \\ &\leq 5.8 + \sqrt{1 + \alpha} \end{aligned} \tag{54}$$

We have chosen $K = 1$ and $\lambda = 0.5$ because the values of K and λ must satisfy $K > 0$ and $0 < \lambda < 1$ and they determine the finite convergence time given by (18). Then, using (45), (53) and (54) we have

$$|d^{\pm}| \leq 8.36 + 2.3\alpha + 3\alpha^2 + \sqrt{1 + \alpha} + 0.08\frac{1}{\alpha} + 0.01\frac{1}{\alpha^2} \tag{55}$$

Let us choose α, such that

$$|d^{\pm}| \leq -1 + 5\pi \tag{56}$$

so that $d^{\pm}$ will be in the range of $g(u)$. The value $\alpha = 0.94$ satisfies this criterion.

With this choice of K, α and λ, the requirements of (27) are satisfied, therefore we can use this law to control the given system. Table 1 gives the values of parameters that were used for numerical simulation.

D. SIMULATION RESULTS

We check the performance of the control loop using numerical simulation.

The reference acceleration is depicted in figure 4 and the initial reference speed and position are $\dot{r}(0) = -1$ and $r(0) = -1$, respectively. The initial speed and position of the system are both 0, i.e. $\dot{x}(0) = 0$ and $x(0) = 0$.

Figure 5 demonstrates the controller's position tracking capability. The time t_s is the terminal reaching time given by (18) and $\frac{4}{\alpha}$ is four times the time constant $\frac{1}{\alpha}$ that the system acquires after the reaching phase ends.

Figure 6 depicts the position error $e(t) = r(t) - x(t)$ of the system. Note that the band $\langle -\Delta/\alpha, \Delta/\alpha \rangle$ is where $e(t)$ converges with the time constant $\frac{1}{\alpha}$ after the reaching phase ends, see (35).

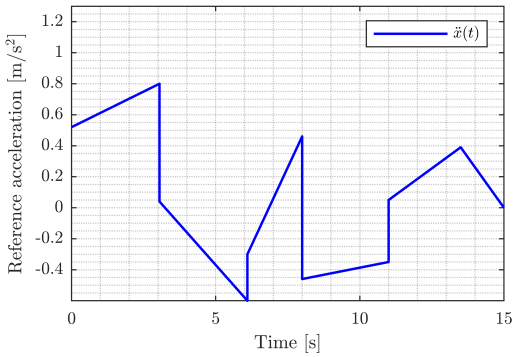

FIGURE 4. The reference acceleration $\ddot{r}(t)$.

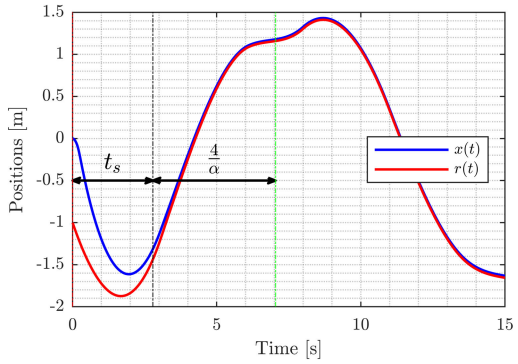

FIGURE 5. The system position $x(t)$ and the reference signal $r(t)$ for the first numerical experiment.

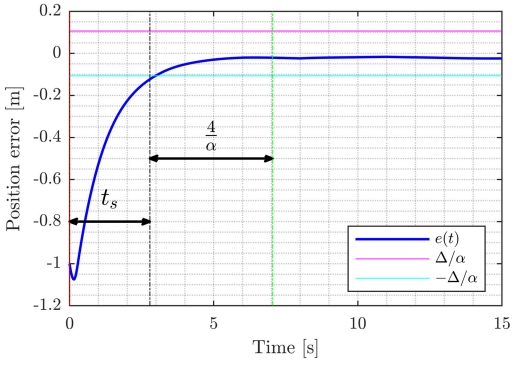

FIGURE 6. The position error $e(t) = r(t) - x(t)$.

The system speed and the reference speed are shown in figure 7. Observe, that the system speeds overshoots the reference speed in order to "catch up" with the reference position.

Figure 8 shows the speed error $\dot{e}(t) = \dot{r}(t) - \dot{x}(t)$. It converges with the time constant $\frac{1}{\alpha}$ into the band $\langle -2\Delta, 2\Delta \rangle$ after the reaching phase ends $t > t_s$.

Figure 9 depicts the control effort $u(t)$ and the more detailed view of control effort transition around the time 3.05 can also be seen in figure 9.

The evolution of the sliding function value $s(\boldsymbol{e})$ appears in figure 10. Note that after the reaching phase ends, the value of $s(\boldsymbol{e})$ has already converged into the band $\langle -\Delta, \Delta \rangle$.

The disturbance signal $\eta(t)$ and the input function uncertainty $\kappa(t)$ are in figure 11.

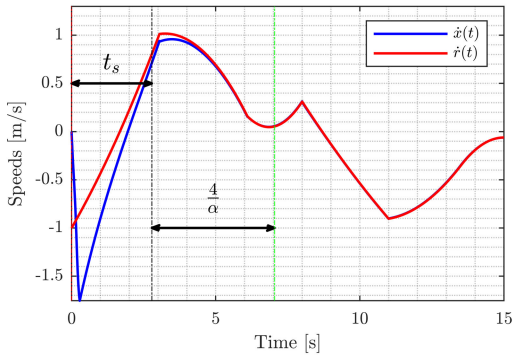

FIGURE 7. The system speed $\dot{x}(t)$ and the reference speed $\dot{r}(t)$.

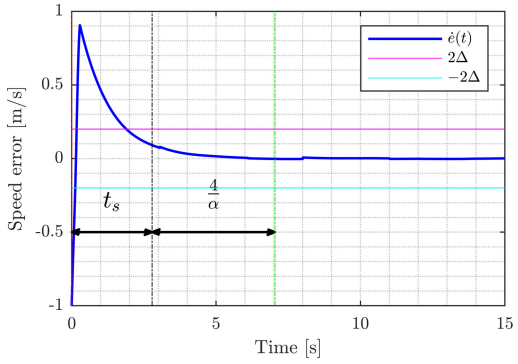

FIGURE 8. The speed error $\dot{e}(t) = \dot{r}(t) - \dot{x}(t)$.

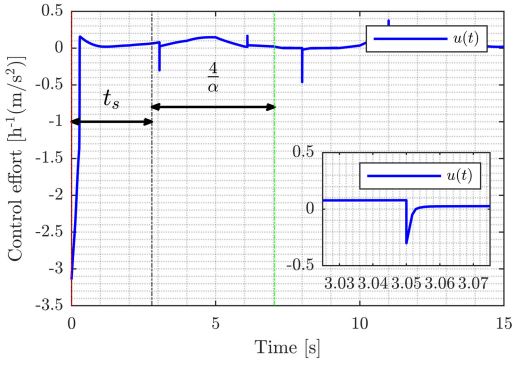

FIGURE 9. The control effort $u(t)$.

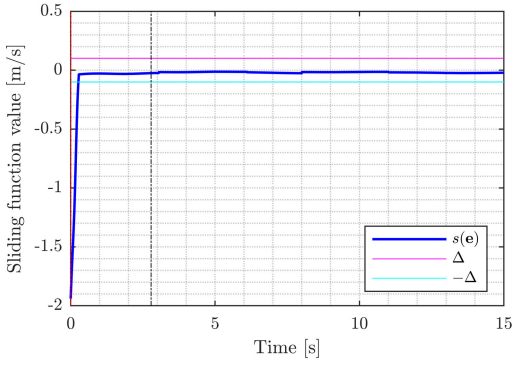

FIGURE 10. The sliding function value $s(e)$.

Figure 12 depicts the system's trajectory $\boldsymbol{e}(t)$ in state (error) space $E = (e(t), \dot{e}(t))$. The switching manifold $s(\boldsymbol{e}) = 0$ is also shown in this figure. As previously noted, the value of

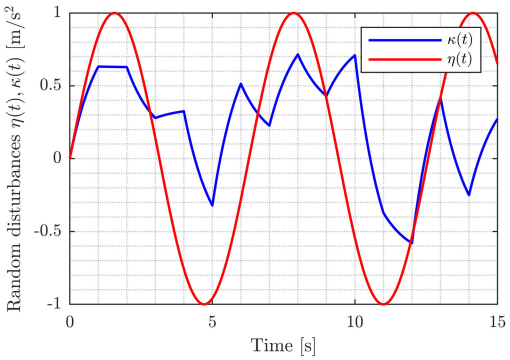

FIGURE 11. The disturbance $\eta(t)$ and the input function uncertainty $\kappa(t)$.

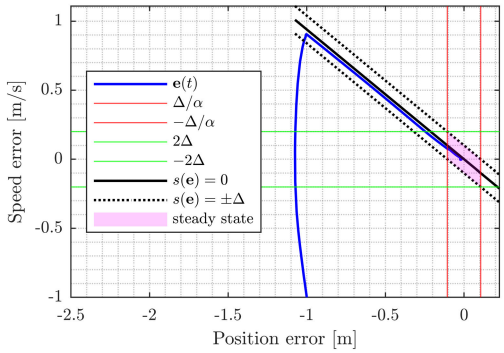

FIGURE 12. The system's state (error) space trajectory $e(t)$ and the steady state region.

the switching function $s(\boldsymbol{e})$ stays within the interval $\langle -\Delta, \Delta \rangle$ after the reaching phase ends. The boundary manifolds $s(\boldsymbol{e}) = \pm\Delta$ are also shown. The system state $\boldsymbol{e}(t)$ converges into the steady state region, which is the pink region in 12.

The performance of the controller depends on the reaching law (17) and the compensated dynamics (22). Figure 10 shows that the actual reaching time is lower than (18), this is do to the disturbance margins η_{max} and ξ_{max} hastening convergence. However, making these margins excessively large can induce chattering in real systems.

VIII. CONCLUSION

In this paper, we apply variable structure control theory to control nonlinear second order systems, where the functional relation of the system acceleration and the control input is nonlinear, discontinuous and uncertain. We refer to this relation as the input function.

The nonlinear discontinuous and uncertain input function is divided into an invertible part and a bounded error part. The difference between the real non-invertible input function and the invertible approximation is then suppressed by the disturbance rejection property of variable structure control.

We design a finite time reaching and exponential sliding mode controller and verify its performance. The controller performed well and satisfied the specified criteria.

REFERENCES

[1] M. A. Sepestanaki, M. H. Barhaghtalab, S. Mobayen, A. Jalilvand, A. Fekih, and P. Skruch, "Chattering-free terminal sliding mode control based on adaptive barrier function for chaotic systems with unknown uncertainties," *IEEE Access*, vol. 10, pp. 103469–103484, 2022.

[2] S. Wu, X. Su, and K. Wang, "Time-dependent global nonsingular fixed-time terminal sliding mode control-based speed tracking of permanent magnet synchronous motor," *IEEE Access*, vol. 8, pp. 186408–186420, 2020.

[3] R. Ma, G. Zhang, and O. Krause, "Fast terminal sliding-mode finite-time tracking control with differential evolution optimization algorithm using integral chain differentiator in uncertain nonlinear systems," *Int. J. Robust Nonlinear Control*, vol. 28, no. 2, pp. 625–639, Jan. 2018.

[4] N. Nguyen, H. T. Nguyen, and S. Su, "Neuro-sliding mode multivariable control of a powered wheelchair," in *Proc. 30th Annu. Int. Conf. IEEE Eng. Med. Biol. Soc.*, Aug. 2008, pp. 3471–3474.

[5] E. Kayacan, "Sliding mode learning control of uncertain nonlinear systems with Lyapunov stability analysis," *Trans. Inst. Meas. Control*, vol. 41, no. 6, pp. 1750–1760, Apr. 2019.

[6] Y. Yildiz, A. Sabanovic, and K. Abidi, "Sliding-mode neuro-controller for uncertain systems," *IEEE Trans. Ind. Electron.*, vol. 54, no. 3, pp. 1676–1685, Jun. 2007.

[7] X. Yu, Y. Feng, and Z. Man, "Terminal sliding mode control—An overview," *IEEE Open J. Ind. Electron. Soc.*, vol. 2, pp. 36–52, 2021.

[8] M. Zhihong, A. P. Paplinski, and H. R. Wu, "A robust MIMO terminal sliding mode control scheme for rigid robotic manipulators," *IEEE Trans. Autom. Control*, vol. 39, no. 12, pp. 2464–2469, Dec. 1994.

[9] S. P. Bhat and D. S. Bernstein, "Finite-time stability of homogeneous systems," in *Proc. Amer. Control Conf.*, vol. 4, Jun. 1997, pp. 2513–2514.

[10] Y. Shtessel, C. Edwards, L. Fridman, and A. Levant, *liding Mode Control and Observation* (Control Engineering). New York, NY, USA: Springer, 2013.

[11] M.-S. Chen, Y.-R. Hwang, and M. Tomizuka, "A state-dependent boundary layer design for sliding mode control," *IEEE Trans. Autom. Control*, vol. 47, no. 10, pp. 1677–1681, Oct. 2002.

[12] E. Herman and G. Strang, *Calculus* (Open Textbook Library), vol. 2. Houston, TX, USA: OpenStax, Rice Univ., 2016.

DENIS VASKO was born in Slovakia, in 1997. He received the Bachelor of Science degree and the Master of Science degree in cybernetics from the Faculty of Electrical Engineering and Information Technology, Slovak University of Technology in Bratislava, in 2019 and 2021, respectively, where he is currently pursuing the Ph.D. degree. His research interests include variable structure control methods, lyapunov design approach, and soft computing.

JÁN KARDOŠ received the M.S. and Ph.D. degrees in cybernetics and automation from the Slovak University of Technology in Bratislava, Slovakia, in 1976 and 2004 respectively. Since 2012, he has been an Assistant Professor with the Faculty of Electrical Engineering and Information Technology, Institute of Robotics and Cybernetics, Slovak University of Technology. His research interests include the theory of control in robotics and mechatronics, particularly the robust variable structure control of motion systems and the modeling and control of the biologically inspired systems.

EVA MIKLOVIČOVÁ received the M.Sc. and Ph.D. degrees in automation both from the Slovak University of Technology (STU) in Bratislava, in 1990 and 1997, respectively. Currently, she is with the Faculty of Electrical Engineering and Information Technology, Institute of Robotics and Cybernetics, STU in Bratislava, as an Associate Professor. Her research interests include predictive control, adaptive control, system modeling, and identification.